

The Role of Adenine Excimers in the Photophysics of Oligonucleotides

Gloria Olaso-González, Manuela Merchán, and Luis Serrano-Andrés*

Instituto de Ciencia Molecular, Universitat de València, Apartado 22085, ES-46071 Valencia, Spain

Received October 27, 2008; E-mail: Luis.Serrano@uv.es

Abstract: Energies and structures of different arrangements of the stacked adenine homodimer have been computed at the ab initio CASPT2 level of theory in isolation and in an aqueous environment. Adenine dimers are shown to form excimer singlet states with different degrees of stacking and interaction. A model for a 2-fold decay dynamics of adenine oligomers can be supported in which, after initial excitation in the middle UV range, unstacked or slightly stacked pairs of nucleobases will relax by an ultrafast internal conversion to the ground state, localizing the excitation in the monomer and through the corresponding conical intersection with the ground state. On the other hand, long-lifetime intrastrand stacked excimer singlet states will be formed in different conformations, including neutral and charge transfer dimers, which originate the red-shifted emission observed in the oligonucleotide chains and that will evolve toward the same monomer decay channel after surmounting an energy barrier. By computing the transient absorption spectra for the different structures considered and their relative stability in vacuo and in water, it is concluded that in the adenine homodimers the maximum-overlap face-to-face orientations are the most stable excimer conformations observed in experiment.

Introduction

Because of the growing concern about the role of solar UV light on human health, the study of DNA's behavior against such type of radiation is an area of increasing research.^{1–6} The excited-state nature of DNA and its nucleobase multimers is complex and depends on conformation and base sequence.^{3,7–13} The absorption spectrum of DNA closely resembles that of the building-block monomers. The low-lying excited states of nucleic acid base (NAB) monomers are accessible by middle UV absorption, near 5 eV,^{3–5,12} and have extremely short lifetimes, in the sub-picosecond regime, due to the presence of ultrafast internal conversions channels toward the ground state,

displaying just a very weak emission ($\tau_i = 10^{-4}$) measured in polar solvents.^{3,9,11} In the multimers, however, the fluorescence spectrum is characterized for having an additional longer-decay component, red-shifted with respect to that of the constituent nucleotides. The slow relaxation channels have been measured in a variety of oligonucleotides by different techniques, such as time- and wavelength-resolved fluorescence^{11,14} and femto-second excited-state absorption (fs-ESA),^{7,11,15,16} although the nature of the decay is still under debate.^{15,17} The origin of the long-decay channels is nowadays attributed to the existence of excimer or exciplex states of pairs of π -stacked nucleobases (homodimer or heterodimer, respectively), a concept that was first used by Eisinger et al.¹³ to describe the observed red-shifted emission as being an excimer fluorescence, and has been firmly established at a theoretical ab initio level.¹⁸

The most recent accounts^{15,16} suggest that after initial radiative population of delocalized exciton states on the NAB multimers, the system evolves in an ultrafast manner to either a fluorescent excimer/exciplex state or a localized excited-state of the NAB monomer, depending on the larger or smaller degree of stacking, respectively. From the long-lived excimer/exciplex state, the system is expected to decay to the ground-state slowly ($\tau > 10$ ps), while the relaxation along the monomer path should

- (1) Callis, P. R. *Annu. Rev. Phys. Chem.* **1983**, *34*, 329–357.
- (2) Cadet, J.; Vigny, P. In *Bioorganic Photochemistry*; Morrison, H., Ed.; John Wiley & Sons: New York, 1990; Vol. 1, pp 1–272.
- (3) Crespo-Hernández, C. E.; Cohen, B.; Hare, P. M.; Kohler, B. *Chem. Rev.* **2004**, *104*, 1977–2019.
- (4) Serrano-Andrés, L.; Merchán, M.; Borin, A. C. *Proc. Natl. Acad. Sci. U.S.A.* **2006**, *103*, 8691–8696.
- (5) Serrano-Andrés, L.; Merchán, M.; Borin, A. C. *Chem. Eur. J.* **2006**, *12*, 6559–6571.
- (6) Roca-Sanjuán, D.; Olaso-González, G.; González-Ramírez, I.; Serrano-Andrés, L.; Merchán, M. *J. Am. Chem. Soc.* **2008**, *130*, 10768–10779.
- (7) Crespo-Hernández, C. E.; Kohler, B. *J. Phys. Chem. B* **2004**, *108*, 11182–11188.
- (8) Crespo-Hernández, C. E.; Cohen, B.; Kohler, B. *Nature* **2005**, *436*, 1141–1144.
- (9) Schreier, W. J.; Schrader, T. E.; Soller, F. O.; Gilch, P.; Crespo-Hernández, C. E.; Swaminathan, V. N.; Carell, T.; Zinth, W.; Kohler, B. *Science* **2007**, *315*, 625–629.
- (10) Holman, M. R.; Ito, T.; Rokita, S. E. *J. Am. Chem. Soc.* **2007**, *129*, 6–7.
- (11) Kwok, W.-M.; Ma, C.; Phillips, D. L. *J. Am. Chem. Soc.* **2006**, *128*, 11894–11905.
- (12) Eisinger, J.; Shulman, R. G. *Science* **1968**, *161*, 1311–1319.
- (13) Eisinger, J.; Guéron, M.; Shulman, R. G.; Yamane, T. *Proc. Natl. Acad. Sci. U.S.A.* **1966**, *55*, 1015–1020.

- (14) Plessow, R.; Brockhinke, A.; Eimer, W.; Kohse-Höinghaus, K. *J. Phys. Chem. B* **2000**, *104*, 3695–3704.
- (15) Crespo-Hernández, C. E.; De La Harpe, K.; Kohler, B. *J. Am. Chem. Soc.* **2008**, *130*, 10844–10845.
- (16) Takaya, T.; Su, C.; De La Harpe, K.; Crespo-Hernández, C. E.; Kohler, B. *Proc. Natl. Acad. Sci. U.S.A.* **2008**, *105*, 10285–10290.
- (17) Miannay, F.-A.; Banyasz, A.; Gustavsson, T.; Markovitsi, D. *J. Am. Chem. Soc.* **2007**, *129*, 14574–14575.
- (18) Olaso-González, G.; Roca-Sanjuán, D.; Serrano-Andrés, L.; Merchán, M. *J. Chem. Phys.* **2006**, *125*, 231102.

be ultrafast ($\tau < 2$ ps), as known in the isolated systems.^{3,19} It has been claimed that the excimer/exciple state has a charge transfer (CT) nature and that there exists a correlation between the state lifetime and the driving force for charge recombination.¹⁶ The formation and quenching of bonded exciplex CT states has been also described between pyridine and cyanoaromatic electron acceptors as a new form of photochemical reaction.²⁰ The fate of the excited state will be strongly dependent on the extent of charge reorganization between the monomers and the relative energetic position of the CT and non-CT excimer states, information that can be obtained from theory. In the case of DNA, dynamics validation of the model only relies on a theoretical time-dependent density functional theory (TD-DFT) report of adenine and 9-methyladenine dimers and trimers in which the CT states were obtained as the low-lying excimer states in solution.²¹ The results of the TD-DFT methodology in calculations that simultaneously involve CT and non-CT excited states must always be taken with great caution because of the well-known tendency of TD-DFT toward severe underestimation of CT excitation energies.^{22–25} Particularly in this case, a recently published study²⁶ suggests that the mentioned TD-DFT report underestimated the CT excitation energies by near 1 eV. It is clear that there is a need of having theoretical studies at higher levels of theory. In the present paper we will focus our interest on the analysis of the excited electronic states responsible for the spectroscopic properties for different adenine (9H-adenine, A) dimer arrangements in vacuo and in an aqueous environment. The relative positions and binding energies of the excimer states, excitation energies, and oscillator strengths for transient absorption spectroscopy, and an overall model for the deactivation dynamics of the homodimer, shall be offered. The results, obtained by an accurate quantum-chemical ab initio method, namely the complete active space self-consistent-field second-order perturbation theory (CASPT2),^{27–29} employing high-quality ANO-type basis sets,³⁰ and using the Polarizable Continuum Model (PCM)^{31,32} for solvation effects, are expected to provide the

Table 1. Energies of the Low-Lying Singlet $\pi\pi^*$ Excited States in the 9H-Adenine Monomer Computed at the Ground-State Geometry with Different Basis Sets and Active Spaces

basis set	active space (e ⁻ /MO)	CASPT2 energies (eV)	
6-31G(d,p) ^a	16/13	S ₁	5.16
		S ₂	5.35
6-31G(d) ^b	10/9	S ₁	5.10
		S ₂	5.45
ANO-L C,N[4s3p1d]/H[2s]+1s1p1d ^c	10/10	S ₁	5.13
		S ₂	5.20
ANO-S C,N[3s2p1d]/H[2s1p]	6/6	S ₁	5.25
		S ₂	5.42

^a Values taken from refs 4 and 5. ^b The standard Gaussian-d exponent 0.8 has been replaced by the more diffuse exponent 0.25 in the basis set. See ref 42. ^c Values taken from ref 41.

grounds to establish more complete models to understand DNA relaxation dynamics.

Methods and Computational Details

Characterization of the lowest singlet states of the adenine homodimer in different arrangements has been carried out by using the CASPT2 method as implemented in the MOLCAS 6.3 software.^{33,34} In order to minimize weakly interacting intruder states, the imaginary level-shift technique (0.2 au) was employed.³⁵ The basis set of Atomic Natural Orbital (ANO-S) type with the primitive set C,N(10s6p3d)/H(7s3p),³⁶ contracted to C,N[3s2p1d]/H[2s1p], was used throughout. The CASSCF state interaction (CASSI) method^{37,38} was used to calculate the transition dipole moments. In the expression for the oscillator strength, the CASSCF transition moment and the energy difference obtained in the CASPT2 computation were employed. Considering our interest in the calculation of $\pi\pi^*$ states of the homodimer, the active space for the CASSCF wave functions comprises a total of 12 electrons distributed along 12 π molecular orbitals (MOs), that is CASSCF(12/12), that correspond to 6 MOs of each adenine. Other states, such as $n\pi^*$, will be much higher in energy (because of hydrogen-bond interactions of different types in the DNA strand) and will play a minor role.^{39,40} In order to select the proper basis set and active space, CASPT2 calibration calculations were performed on the low-lying singlet states of the adenine monomer using the optimized CASSCF (11,12)/6-31G(d,p) ground-state geometry obtained by Serrano-Andrés et al.⁵ Table 1 compiles the results of modifying basis sets and active spaces. In particular, the use of the more restricted (6,6) active space for adenine still provides results that are in agreement with the values obtained earlier employing larger active spaces.^{5,41}

For the study of the adenine homodimer, different molecular arrangements were studied in vacuo and in water, employing in

- (19) Serrano-Andrés, L.; Merchán, M. Photostability and Photoreactivity in Biomolecules: Quantum Chemistry of Nucleic Acid Base Monomers and Dimers In *Radiation Induced Molecular Phenomena in Nucleic Acids: A Comprehensive Theoretical and Experimental Analysis*; Shukla, M. K.; Leszczynski, J., Eds.; Springer: The Netherlands, 2008; pp 435–472.
- (20) Wang, Y.; Haze, O.; Dinnocenzo, J. P.; Farid, S. *J. Org. Chem.* **2007**, *72*, 6970–6981.
- (21) Santoro, F.; Barone, V.; Improta, R. *Proc. Natl. Acad. Sci.* **2007**, *104*, 9931–9936.
- (22) Tozer, D. J.; Amos, R. D.; Handy, N. C.; Roos, B. O.; Serrano-Andrés, L. *Mol. Phys.* **1999**, *97*, 859–868.
- (23) Tozer, D. J. *J. Chem. Phys.* **2003**, *119*, 12697.
- (24) Drew, A.; Weisman, J. L.; Head-Gordon, M. *J. Chem. Phys.* **2003**, *119*, 2943.
- (25) Lange, A.; Herbert, J. M. *J. Chem. Theory Comput.* **2007**, *3*, 1680–1690.
- (26) Lange, A. W.; Rohrdanz, M. A.; Herbert, J. M. *J. Phys. Chem. B* **2008**, *112*, 6304–6308.
- (27) Andersson, K.; Malmqvist, P.-Å.; Roos, B. O. *J. Chem. Phys.* **1992**, *96*, 1218–1226.
- (28) Roos, B. O.; Andersson, K.; Fülischer, M. P.; Malmqvist, P.-Å.; Serrano-Andrés, L.; Pierloot, K.; Merchán, M. *Adv. Chem. Phys.* **1996**, *93*, 219–331.
- (29) Merchán, M.; Serrano-Andrés, L. In *Computational Photochemistry*; Olivucci, M., Ed.; Elsevier: Amsterdam, 2005; pp 35–91.
- (30) Serrano-Andrés, L.; Merchán, M. *J. Mol. Struct. (THEOCHEM)* **2005**, *729*, 99–108.
- (31) Cossi, M.; Barone, V. *J. Chem. Phys.* **2001**, *115*, 4708–4717.
- (32) Tomasi, J.; Mennucci, B.; Cammi, R. *Chem. Rev.* **2005**, *105*, 2999–3094.

- (33) Karlström, G.; Lindh, R.; Malmqvist, P.-Å.; Roos, B. O.; Ryde, U.; Veryazov, V.; Widmark, P.-O.; Cossi, M.; Schimmelpfennig, B.; Neogady, P.; Seijo, L. *Comput. Mater. Sci.* **2003**, *28*, 222–239.
- (34) Veryazov, V.; Widmark, P.-O.; Serrano-Andrés, L.; Lindh, R.; Roos, B. O. *Int. J. Quantum Chem.* **2004**, *100*, 626–635.
- (35) Forsberg, N.; Malmqvist, P.-Å. *Chem. Phys. Lett.* **1997**, *274*, 196–204.
- (36) Pierloot, K.; Dumez, B.; Widmark, P.-O.; Roos, B. O. *Theor. Chim. Acta* **1995**, *90*, 87–114.
- (37) Malmqvist, P.-Å. *Int. J. Quantum Chem.* **1986**, *30*, 479–494.
- (38) Malmqvist, P.-Å.; Roos, B. O. *Chem. Phys. Lett.* **1989**, *155*, 189–194.
- (39) Ritzke, H.-H.; Hobza, P.; Nachtigallova, D. *Phys. Chem. Chem. Phys.* **2007**, *9*, 1672–1675.
- (40) Serrano-Andrés, L.; Fülischer, M. P.; Karlström, G. *Int. J. Quantum Chem.* **1997**, *65*, 167–181.
- (41) Fülischer, M. P.; Serrano-Andrés, L.; Roos, B. O. *J. Am. Chem. Soc.* **1997**, *119*, 6168–6176.
- (42) Roca-Sanjuán, D.; Rubio, M.; Merchán, M.; Serrano-Andrés, L. *J. Chem. Phys.* **2006**, *125*, 084302.

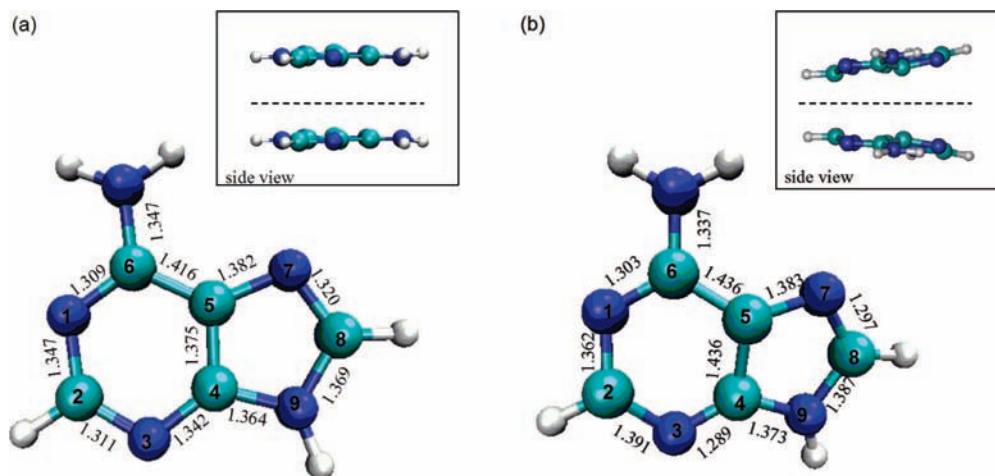


Figure 1. Labeling for the adenine molecule. Structure a corresponds to the ground-state equilibrium geometry of the monomer computed by Serrano-Andrés et al.⁵ and b to the adenine dimer at the optimized $^1(A^*A)_{exc}$ S_1 state. Main bond distances are displayed in angstroms. The inset of part a illustrates the parallel face-to-face arrangement of the adenine dimer, whereas the inset of part b illustrates the orientation in the optimized $^1(A^*A)_{exc}$ state face-to-face minimum.

the latter case the PCM model^{31,32} as implemented in the MOLCAS package.^{33,34} A reaction field approach uses a polarizable dielectric continuum outside a properly shape-adapted cavity to account for the most relevant solvation effects, in an aqueous medium here, and is computed in a multiconfigurational self-consistent manner at the CASSCF level and added to the Hamiltonian as a perturbation, defining the CASPT2/PCM approach. The employed model (see Supporting Information) is considered sufficient to incorporate the main solvation effects on the ground and $\pi\pi^*$ excited states of the adenine dimer.

At this level of theory, different sets of calculations were performed with six different molecular arrangements of the adenine homodimer: a face-to-face symmetric orientation using ground-state optimized monomers, the dimer locally excited state $^1(LE)$ inspired in the homologous cytosine homodimer;⁶ the B-DNA A-dimer arrangement, also using ground-state optimized monomers (B-DNA); an excited-state optimized face-to-face excimer, $^1(A^*A)_{exc}$; two B-DNA orientations including individually optimized cationic and anionic A monomers, ($^sA_{cat}A_{an}^3$) and ($^sA_{an}A_{cat}^3$), and finally an adapted TD-DFT CT excited-state optimized minimum from ref 21 ($^1(A^+A^-)_{opt}$, see below). A different number of roots, seven unless indicated, were used in the average procedure of the CASSCF method to account for the change of order between the CASSCF and the CASPT2 solutions. Except when mentioned, no symmetry restrictions have been used in the calculations. In some cases, as indicated, at specific geometries of the S_1 state, 30 singlet roots were computed at the CASPT2 level in order to explore the measured transient excited-state absorption. As shown previously,^{6,18,43} inclusion of the basis set superposition error (BSSE) is crucial to accurately describe the binding energies (E_b) and relative position of the excimer states. Here the effect was taken into account by using the counterpoise correction (CP)⁴⁴ (see Supporting Information), and the corresponding energies, the only ones used in the discussion, will be named BSSE-corrected or CP-corrected (e.g., CP-corrected binding energy, CP- E_b). Additional computational details and the employed geometries can be found in the Supporting Information.

Results and Discussion

Femtosecond excited-state absorption (fs-ESA) experiments^{7,8,16} carried out on a variety of synthetic DNA oligonucleotides in aqueous solution, for instance (dA)₁₈, obtained multiexponential

decays including relaxation lifetimes between 10 and 100 ps that were attributed to decay from singlet excimers. It was suggested that, after pump absorption at 266 nm, a high yield of the absorbed photons generates excimers whose transient decays at the probe pulse 250 nm (used to reveal ground-state reconstitution) in lock step with the signal at 570 nm (used for probing the excited state) at times greater than 10 ps repopulating the ground state. An additional time-resolved study¹¹ on (dA)₂₀ provided evidence for temporal evolution from three distinct states, the first of them characterized by ultrafast relaxation with a ~ 0.39 ps of decay time, assigned to a monomer-like relaxation, and the second and third ones displaying relatively long-lived states with ~ 4.3 ps and ~ 182 ps lifetimes, respectively, suggested to be originated from excimers. In order to determine the nature and relative position of the different excimer states of the A homodimer in the gas phase and solution, different molecular arrangements of the stacked dimer have been studied at the CASPT2 and CASPT2/PCM level of theory.

A. The Lowest Singlet State in the Parallel Excimer: $^1(LE)$. As a first step toward the characterization of the low-lying singlet excimers of adenine, the potential energy curves (PECs) with respect to the intermolecular mass-center separation (R) of two adenine molecules kept at the ground-state equilibrium geometry have been built at the CASPT2 level. The selected orientation is a symmetric face-to-face parallel arrangement of the A-dimer (see Figure 1), which leads to the maximum overlap and interaction between the π systems of the monomers. Although this homodimer displays spatial C_2 symmetry, we use no symmetry restrictions (C_1 symmetry) in the computation of the electronic state energies to avoid the problems related to wave function symmetry breaking.⁴⁵

Hereafter, relative energies will be referred to two ground-state isolated adenine molecules. In the asymptotic limit S_1 and S_2 become degenerate. They are related to the equivalent situations $A + A^*$ and $A^* + A$, where A and A^* represent the ground-state adenine and its lowest singlet excited state, respectively. Thus, the absorption $S_0 \rightarrow S_1$ calculated with the monomers separated 20 au corresponds to the monomer

(43) Olaso-González, G.; Merchán, M.; Serrano-Andrés, L. *J. Phys. Chem. B* **2006**, *110*, 24734–24739.

(44) Boys, S. F.; Bernardi, F. *Mol. Phys.* **2002**, *100*, 65–73.

(45) Merchán, M.; Pou-AméRigo, R.; Roos, B. O. *Chem. Phys. Lett.* **1996**, *252*, 405–414.

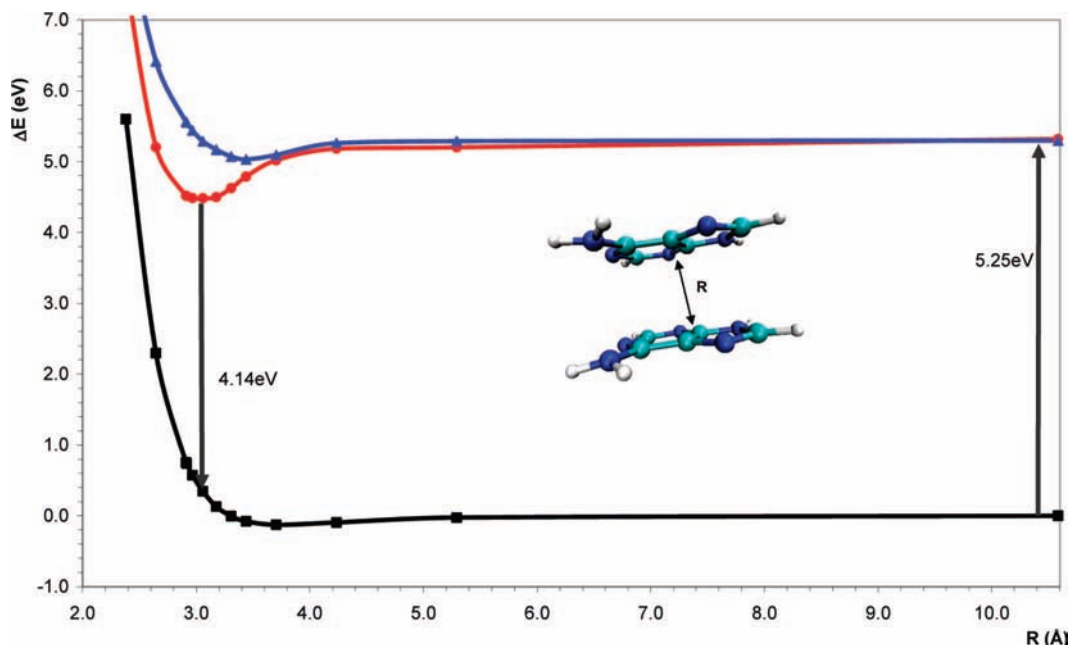


Figure 2. BSSE-corrected CASPT2 potential energy curves built with respect to the intermolecular distance (R) of two face-to-face π -stacked adenine molecules. The curves correspond (in increasing energy order) to the singlet S_0 , S_1 , and S_2 states.

absorption, and it is here computed at 5.25 eV in agreement with previous findings, as can be seen in Table 1. When the two molecules are constrained to be parallel, the PEC for the ground state at the CASPT2 (12/12) level is weakly bound (see Figure 2) having a binding energy of 0.13 eV with a minimum at the intermolecular distance of 3.704 Å. We have a well-defined minimum for S_1 at 3.059 Å with a binding energy (CP- E_b) of 0.83 eV. The S_2 electronic state is bound with a binding energy of 0.27 eV at an intermonomer distance of 3.440 Å. At that local S_1 minimum, hereafter $^1(\text{LE})$, the computed vertical emission energy, 4.14 eV, is 0.3–0.4 eV lower than the measured monomer fluorescence,^{5,46–50} and it can be related to the red-shifted fluorescence observed in adenine oligonucleotides,¹¹ supporting the excimer origin of such emission, whose energy and quantum yield will depend on the secondary structure of the single-stranded polymer.⁷ The pronounced S_2 – S_1 gap points out an efficient coupling between the two states, as previously noted for related systems.³⁹ At this point, the existence of adenine excimers is predicted, and it can be regarded as an intrinsic property of the A-dimer, as determined for other pyrimidine NABs dimers.^{6,18,19,51,52}

Figure 2 contains the PECs for the face-to-face symmetric display. The correction of the BSSE is essential for the accurate calculation of the binding energies and to account for the relative position of the different excimer states, even if the vertical

energy values are barely affected. The BSSE-uncorrected A-dimer PECs have been included in the Supporting Information. The most important difference is that the electronic states lose a high percentage of binding character when the BSSE is taken into consideration. Actually, S_0 and S_2 have well defined minima in the uncorrected PECs, and S_1 has a binding energy of 2.17 eV, 1.34 eV larger than for the CP corrected curve, which also decreases the intermolecular distance for the S_1 minimum in 0.144 Å. In fact, the S_0 state becomes unbound at the $^1(\text{LE})$ structure, lying at 0.25 eV from the reference isolated systems.

B. The Relaxed Singlet Excimer State: $^1(\text{A}^*\text{A})_{\text{exc}}$. Another conformation for the homodimer has been obtained by performing a geometry optimization of the lowest singlet state of the adenine dimer, initially performed within the constraints of the C_s symmetry, in which the lowest-energy state at the CASPT2 level corresponds to the first root of A'' symmetry. The same 12/12 active space has been employed, distributed in six π -active MOs in each of the irreducible representations a' and a . At the optimized geometry, the electronic singlet states have been computed without symmetry restrictions. The relaxed singlet excimer $^1(\text{A}^*\text{A})_{\text{exc}}$, whose CASSCF optimized geometry is represented in Figures 1 and 3, has a binding energy (CP- E_b) of 1.23 eV, and it is stabilized 0.40 eV from the $^1(\text{LE})$ excimer structure. The interaction between the two moieties is the highest because the system remains fully stacked and the intermonomer distance decreases, in particular between the C_5 – C_5' atoms. The interaction between the two moieties also produces the elongation of the C_4 – C_5 (C_4' – C_5') monomer bond, which loses the double bond character. The S_2 state at the $^1(\text{A}^*\text{A})_{\text{exc}}$ geometry has a CP- E_b of just 0.01 eV, whereas the S_2 – S_1 splitting is 1.74 eV, considerably larger than in the other situations studied. That reflects a strong coupling between the states. The vertical transitions toward the ground state are computed to be 2.65 and 4.37 eV for S_1 and S_2 , respectively, and are strongly red-shifted as compared to the lowest vertical singlet–singlet transition of the adenine monomer in solution (4.5 eV).⁵ As in the $^1(\text{LE})$

(46) Plützer, C.; Nir, E.; de Vries, M. S.; Kleinermaans, K. *Phys. Chem. Chem. Phys.* **2001**, *3*, 5466–5469.

(47) Kim, N. J.; Jeong, G.; Kim, Y. S.; Park, Y. D. *J. Chem. Phys.* **2000**, *113*, 10051–10055.

(48) Lührs, D. C.; Viallon, J.; Fischer, I. *Phys. Chem. Chem. Phys.* **2001**, *3*, 1827–1831.

(49) Nir, E.; Plützer, C.; Kleinermaans, K.; de Vries, M. S. *Eur. Phys. J. D* **2002**, *20*, 317–329.

(50) Kim, N. J.; Kang, H.; Park, Y. D.; Kim, S. K. *Phys. Chem. Chem. Phys.* **2004**, *6*, 2802–2805.

(51) Serrano-Pérez, J. J.; González-Ramírez, I.; Coto, P. B.; Merchán, M.; Serrano-Andrés, L. *J. Phys. Chem. B* **2008**, *112*, 14096–14098.

(52) González-Ramírez, I.; Climent, T.; Serrano-Pérez, J. J.; González-Luque, R.; Merchán, M.; Serrano-Andrés, L. *Pure Appl. Chem.* **2009**, in press.

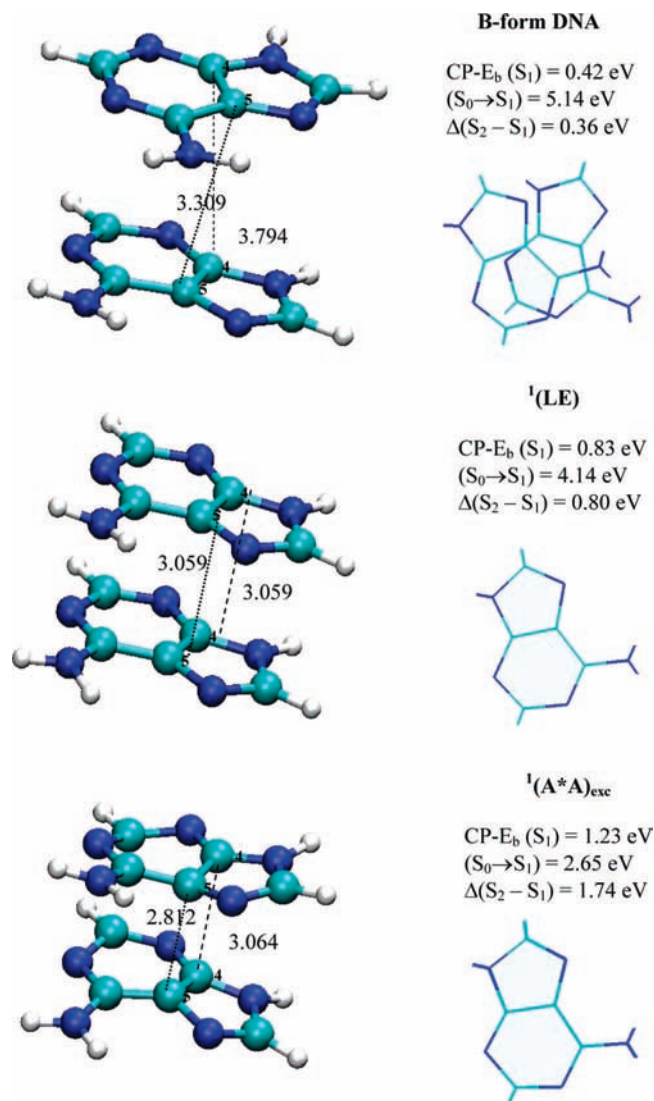


Figure 3. Structures for two adenine molecules: (a) at the ground-state B-form DNA; (b) at the S_1 locally excited state $^1(\text{LE})$ -type structure in a symmetric face-to-face orientation; (c) at the optimized minimum of S_1 (also face-to-face orientation; see text). The computed CASPT2 binding energies ($CP-E_b$) for S_1 , and the vertical transition energy ($S_0 \rightarrow S_1$), together with the splitting for the two lowest excited states, $\Delta(S_2 - S_1)$, are also included. Interatomic distances in angstroms. On the right is shown the overlap between the two moieties in the different structures.

conformation, the ground state is clearly unbound, displaying a relative energy of 1.37 eV above the reference isolated molecules. The dissociative character of the ground states speaks in favor of the arrangement as a source of unstructured red-shifted emission.

C. The Lowest Singlet State in the B-Type DNA Conformation. The low-lying singlet states of the adenine dimer have been also studied in a conformation in which the relative orientation of the ground-state optimized monomers uses the standard parameters of the B-form of DNA.⁵³ This model is mainly characterized by a twist angle of 36° between the two members of the dimer. Figure 3 compiles the relative orientations and the CASPT2 energy bindings, vertical excitations, and excited state splitting for different arrangements of the adenine homodimer.

As can be readily seen from the molecular drawing, the ground-state stacking in the B-form is somewhat different from the symmetric face-to-face (or “sandwich”-like) geometries required for producing the $^1(\text{LE})$ and optimized $^1(\text{A}^*\text{A})_{\text{exc}}$ energy minima, conceived to maximize the stacking interaction. In the ground-state B-form DNA, the interatomic distances $R(\text{C}_4-\text{C}_4')$ and $R(\text{C}_5-\text{C}_5')$ are about 3.309 and 3.794 Å, respectively, both larger than those in $^1(\text{LE})$, at 3.059 Å, whereas the dihedral angle $\angle \text{C}_4-\text{C}_5-\text{C}_5'-\text{C}_4'$, varies from 36° in B-DNA to 0° in $^1(\text{LE})$ and $^1(\text{A}^*\text{A})_{\text{exc}}$. The lowest singlet excited state in the B-form has a binding energy ($CP-E_b$) of 0.42 eV, being therefore 0.41 and 0.81 eV less stable than the $^1(\text{LE})$ and $^1(\text{A}^*\text{A})_{\text{exc}}$ forms, respectively. The S_2-S_1 splitting is also smaller for the B-DNA arrangement, reflecting a weaker coupling between the states. The vertical transitions in the B-DNA dimer, 5.14 eV (S_1) and 5.50 eV (S_2), are slightly blue-shifted as compared to the lowest vertical singlet-singlet transition of $^1(\text{LE})$. At the same level of theory, the ground state in the B-form is computed to be slightly bound, displaying a corrected binding energy, $CP-E_b$, of 0.34 eV.

D. Charge Transfer Singlet States. Solvation Effects. The final conformations of the adenine excimer that have been explored concern the location of the intermonomer charge transfer singlet states. In order to find the most favorable structure for this type of state we have used several arrangements. Ground-state geometries corresponding to the adenine cation (A_{cat}) and anion (A_{an}) obtained from previous CASSCF(12/10 $\pi\pi^*$)/ANO-L C,N[4s3p1d]/H[2s1p] calculations^{42,54} were first employed. Using these moieties, two structures with the B-form arrangement have been built: $^5A_{\text{cat}}A_{\text{an}}^{3'}$, in which the A_{cat} monomer is situated in the position that corresponds to the $5'$ extreme of a hypothetical strand of DNA whereas the A_{an} monomer is in the $3'$ extreme, and $^5A_{\text{an}}A_{\text{cat}}^{3'}$, in which the position of the monomers is inverted. As described later, an additional geometry was employed, hereafter $(\text{A}^+\text{A}^-)_{\text{opt}}$, adapted from that optimized for the lowest CT state of the 9-methyladenine dimer by Santoro et al.²¹ at the TD-DFT/PCM/PBE0/6-31G(d) level of calculation. Figure 4 displays the three employed arrangements, whereas Table 2 compiles the vertical excitation energies, relative positions, and nature of the computed singlet excited states for the isolated system and within an aqueous environment.

The calculations performed on the isolated adenine dimers at the CASPT2 level and including correction of the BSSE show CT states that were the fourth ($^5A_{\text{cat}}A_{\text{an}}^{3'}$) and sixth root ($^5A_{\text{an}}A_{\text{cat}}^{3'}$) at the two employed conformations. In the latter arrangement the CT state, with a 59% of CT character, is too high in energy to be competitive with the low-lying neutral singlet excited states. For the $^5A_{\text{cat}}A_{\text{an}}^{3'}$ arrangement, in which we will focus from now on, the lowest CT state (with 80% of CT character) is located at 4.95 eV from the reference system, two isolated adenine molecules, and displays a binding energy of 0.30 eV, even smaller than that found for the lowest excimer state in the B-DNA arrangement. Also, the CT state is almost 1 eV higher than the lowest excimer state $^1(\text{A}^*\text{A})_{\text{exc}}$, as will be discussed later, and it is practically degenerated with other states where the nature of the electronic transition is delocalized or of intermonomer character. In order to analyze the role of a solvated environment in the relative location of the excimer

(53) Lu, X.-J.; Olson, W. K. *Nucleic Acids Res.* **2003**, *31*, 5108–5121.

(54) Roca-Sanjuán, D.; Rubio, M.; Merchán, M.; Serrano-Andrés, L. *J. Chem. Phys.* **2008**, *129*, 095104.

(55) Gagliardi, L.; Lindh, R.; Karlström, G. *J. Chem. Phys.* **2004**, *121*, 4494.

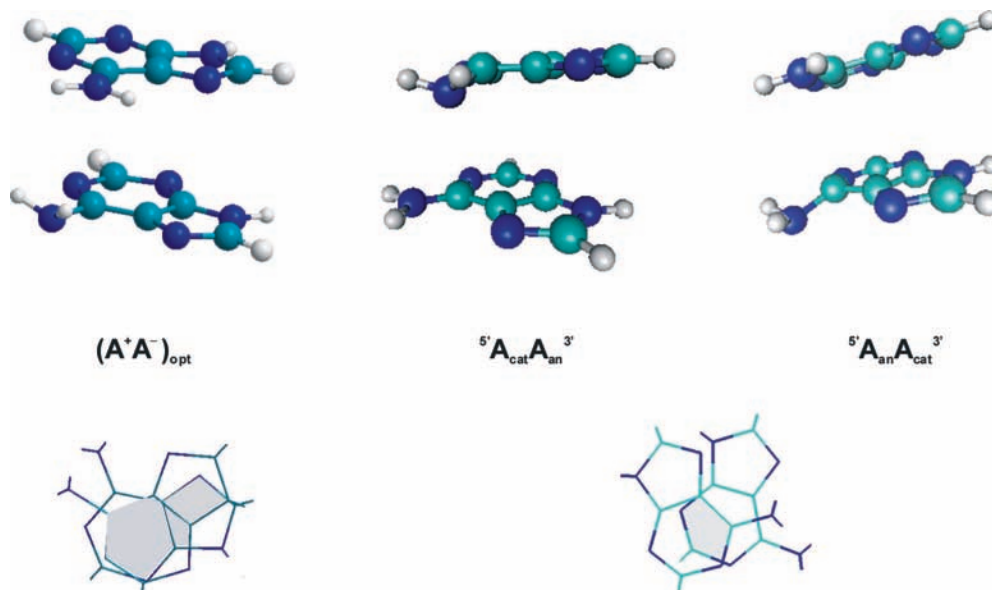


Figure 4. Structures of the studied anionic-cationic arrangement of the adenine dimer and overlap between the two stacked monomers. Whereas the geometry $(A^+A^-)_{opt}$ was adapted from ref 21 (see text), the ground-state optimized geometries for the corresponding anion and cation monomer have been used to build a dimer oriented at a B-DNA conformation. The bottom views show the overlap between the two moieties in the different structures.

Table 2. CASPT2 BSSE-Corrected Vertical (VE) and Relative (to two ground-state isolated monomers, RE) Energies (ΔE /eV) for the Low-Lying Singlet States in the $(A^+A^-)_{opt}$, ${}^5A_{cat}A_{an}{}^{3'}$, and ${}^5A_{an}A_{cat}{}^{3'}$ Structures^a

state	$(A^+A^-)_{opt}{}^b$					${}^5A_{cat}A_{an}{}^{3'}$					${}^5A_{an}A_{cat}{}^{3'}$		
	ΔE				CT ^d nature, %	ΔE				CT ^d nature, %	ΔE , gas phase		
	gas phase		water			gas phase		water			VE ^c	RE	CT ^d nature, %
S ₁	4.42	4.30	4.64	4.26		4.62	4.95	4.31	4.67	80	4.32	4.67	
S ₂	4.60	4.34	4.67	4.29		4.58	4.91				4.61	4.96	
S ₃	4.71	4.38	4.70	4.33		4.61	4.94				4.90	5.25	
S ₄	4.94	4.61	4.77	4.39	34	4.68	5.01				5.49	5.84	
S ₅	5.18	4.85	4.99	4.61	45	5.81	6.14				5.57	5.92	59

^a Also included are results in water at the CASPT2/PCM level and weights of the CT character for the corresponding states. ^b Adapted from ref 21 optimized at the TDDFT level. ^c The ground state is located -0.33 (vapor) and -0.38 eV (water) $(A^+A^-)_{opt}$, 0.33 (vapor) and 0.36 eV (water) $({}^5A_{cat}A_{an}{}^{3'})$, and 0.35 eV $({}^5A_{an}A_{cat}{}^{3'})$ below or above the reference energy (two isolated monomers). ^d Based on LoProp population analysis.⁵⁵ Neutral states have negligible CT character in all cases.

states, we have also performed a number of calculations modeling the solvation effect of an aqueous media by means of the reaction field CASPT2/PCM approach. As observed in Table 2, the CT excimer state stabilizes its energy both vertically and relatively to the separated monomers, in this case down to 4.67 eV, becoming the lowest excited singlet state at such conformation. If compared with the ${}^1(A^*A)_{exc}$, which is placed at 4.02 eV in the gas phase, the CT state is still well above the face-to-face optimized excimer in the adenine homodimer. The ${}^1(A^*A)_{exc}$ S₁ state minimum is computed at 3.95 eV in the aqueous environment, slightly stabilized from the gas-phase value and, in any case, much more stable than the CT state.

Those $A_{cat}A_{an}$ structures were displayed in a B-DNA-type arrangement, which is characterized by having a small overlap of the stacked moieties (see Figures 3 and 4). As the binding energy and relative position of the excimer states strongly depend on the degree of stacking and overlap, we performed additional calculations on a structure with a slightly larger overlap and also optimal for getting CT-type states at low energies (see Figure 4). The geometry we adopted, $(A^+A^-)_{opt}$, was adapted from that optimized for the lowest CT state of the 9-methyladenine dimer by Santoro et al.²¹ at the TD-DFT/PCM/PBE0/6-31G(d) level of calculation. The methyl groups were

replaced by hydrogen atoms with NH bond lengths of 1.00 Å. As described,²¹ the geometries of each one of the moieties resemble those of the anion and cation of the monomer. Independently of the relative position at which the TD-DFT method places the CT states (typically it yields too low excitation energies^{22–26}), a reasonable account of the geometrical parameters can be expected. In any case, we carried out the calculations to analyze different arrangements which might lead to stabilize CT states. Here (cf. Table 2) the lowest CT state at the $(A^+A^-)_{opt}$ geometry was located in the gas phase at higher energies (~ 0.3 eV) than the non-CT states, and only when the solvent is included does it stabilize to become much closer, at 4.39 eV. This relative position is nearly 0.3 eV lower than the value obtained in other conformations. As compared with the CT states found in the other arrangements, the transfer of the charge from one to the other monomer was not so pronounced (34%) in the CASSCF(12/12) wave function. We can therefore conclude that certainly this structure has provided more stable CT excimer states, but they still lie higher than the strongly interacting ${}^1(A^*A)_{exc}$ conformation, even in a polar solvent like water, where the vertical excitation and relative energy of the ${}^1(A^*A)_{exc}$ S₁ minimum lie at 2.58 and 3.95 eV, respectively. This conclusion can be expected to be generally

Table 3. CASPT2 Energy Differences ($\Delta E/eV$) and Oscillator Strengths (f) of the Most Relevant Transitions from the Ground and Singlet Excited States of the Adenine Dimer at Different Conformations^a

B-form			$(A^+A^-)_{opt}^b$			${}^1(LE)$			${}^1(A^*A)_{exc}$		
	ΔE	f		ΔE	f		ΔE	f		ΔE	f
Ground-State Absorption/Emission											
$S_0 \rightarrow S_1$	5.15	0.037	$S_0 \rightarrow S_1$	4.42	0.254	$S_0 \rightarrow S_1$	4.14	0.0001	$S_0 \rightarrow S_1$	2.65	0.011
$S_0 \rightarrow S_2$	5.50	0.072	$S_0 \rightarrow S_2$	4.60	0.009	$S_0 \rightarrow S_2$	4.94	$<10^{-4}$	$S_0 \rightarrow S_2$	4.37	0.028
Excited-State Absorption ^c											
$S_1 \rightarrow S_4$	0.43	0.0015	$S_1 \rightarrow S_5$	0.93	0.0157	$S_1 \rightarrow S_3$	0.92	0.026	$S_1 \rightarrow S_5$	2.18	0.029
$S_1 \rightarrow S_6$	1.03	0.0007	$S_4 \rightarrow S_5$	0.39	0.0221	$S_1 \rightarrow S_{12}$	2.33	0.182	$S_1 \rightarrow S_6$	2.24	0.224
$S_2 \rightarrow S_5$	0.75	0.0187	$S_5 \rightarrow S_{15}^{CT}$	1.72	0.0369	$S_1 \rightarrow S_{13}$	2.34	0.061	$S_1 \rightarrow S_7$	2.52	0.021
$S_2 \rightarrow S_7$	1.13	0.0131	$S_{10}^{CT} \rightarrow S_{17}$	1.02	0.0217	$S_1 \rightarrow S_{18}$	2.88	0.046	$S_1 \rightarrow S_8$	2.60	0.114
$S_2 \rightarrow S_8$	1.32	0.0003	$S_{12} \rightarrow S_{21}^{CT}$	1.06	0.0278	$S_2 \rightarrow S_{12}$	2.09	0.136	$S_1 \rightarrow S_{11}$	2.85	0.133
$S_2 \rightarrow S_{12}$	1.94	0.0015	$S_{14} \rightarrow S_{16}$	0.39	0.0233	$S_2 \rightarrow S_{13}$	2.10	0.054	$S_2 \rightarrow S_{16}$	2.28	0.005
$S_2 \rightarrow S_{13}$	2.10	0.0198	$S_{14} \rightarrow S_{21}^{CT}$	0.97	0.0637	$S_4 \rightarrow S_{15}$	1.75	0.122	$S_2 \rightarrow S_{17}$	2.43	0.134
$S_2 \rightarrow S_{14}$	2.12	0.0126	$S_{16} \rightarrow S_{20}$	0.40	0.0270	$S_5 \rightarrow S_{18}$	1.81	0.131	$S_3 \rightarrow S_{10}$	1.02	0.060
$S_4 \rightarrow S_{19}$	1.95	0.0107	$S_{16} \rightarrow S_{21}^{CT}$	0.57	0.0392	$S_6 \rightarrow S_{17}$	1.70	0.146	$S_3 \rightarrow S_{15}$	2.11	0.027

^a Relative energies of the respective ground states from that of the two separated monomers: -0.34 eV (B-form), -0.33 eV $(A^+A^-)_{opt}$, 0.25 eV $({}^1(LE))$, 1.37 eV $({}^1(A^*A)_{exc})$. ^b Geometry adapted from ref 21 (see text). ^c Only nine transitions with the highest oscillator strengths are shown.

valid for nucleobase homodimers, whereas for heterodimers the strongly stacked neutral states and the CT states could be more competitive.

E. Adenine Dimer Transient Absorption. Crespo-Hernández et al.⁷ recorded the femtosecond transient absorption signal for the DNA oligonucleotide $(dA)_{18}$ in aqueous solution. According to their findings an excited state is rapidly formed after initial excitation that can be assigned to a singlet excimer. Absorption is measured for this state at 570 nm (2.18 eV), which decays in times larger than 10 ps, repopulating the ground state that, in turn, is detected by monitoring its typical strong absorption at 250 nm (4.96 eV). We have computed the transient absorption spectrum for the lowest singlet states in four different conformations. The energies for those transitions with the largest oscillator strengths as well as the energy of the transitions $S_0\Delta S_1$ and $S_0\Delta S_2$ are collected in Table 3. Because of the limitations in the size of the active space, high-lying states may not be accurately represented. The goal of these calculations is, however, to identify species for intense transient absorption near the observed 2.18 eV at the different arrangements. Only singlet excited valence $\pi\pi^*$ states are of interest in that context.

After initial absorption at 266 nm (4.66 eV), probably to produce a delocalized exciton-type situation,⁵⁶ the oligomer strand, which can be assumed in average in a B-form conformation, will evolve toward different excimer-like structures, whose formation yield will strongly depend on the dynamics and flexibility of the strand. Most of the observed excited-state transient absorption will take place at favorable S_1 minima conformations. From the four structures studied here, B-DNA, $(A^+A^-)_{opt}$, ${}^1(LE)$, and ${}^1(A^*A)_{exc}$, the two latter seem to better support the fs-ESA experiment and are good candidates to be assigned as responsible for the red-shifted fluorescence. Both conformations, that highly increase the stability of the lowest singlet excited state, have strong absorptions from the state S_1 to higher states with energies between 2.09–2.33 eV. On the contrary, at the B-form and $(A^+A^-)_{opt}$ structures no strong transient absorption is found near the 2.18 eV experimental signal (strong transient absorption are also reported at higher energies), even when the $(A^+A^-)_{opt}$ conformation displays a reasonable large overlap of the stacked π structures (see Figure 4) which could be expected to enhance the intensity of the absorption bands.^{7,11} According to these findings, the signal

monitored at 570 nm in the transient absorption experiment could be caused by the electronic transition from the S_1 state of the adenine dimer in the favored ${}^1(LE)$ or ${}^1(A^*A)_{exc}$ structures, far from the other conformations, indicating that a relaxation, ultrafast, as suggested,¹⁶ of the dimer structure takes place after the excitation of the DNA with the pump laser and before the excitation with the probe laser. If the two structures are taken as limits for the relaxation process, the fluorescence energy range could be expected between 4.14–2.65 eV, perfectly covering the observed domain, 310–550 nm (4.0–2.3 eV).¹¹ On the other hand, the repopulation of the ground state is monitored thanks to its absorption at 250 nm (4.96 eV), which is close to the $S_0 \rightarrow S_1$ transition to the dimer B-form or to the monomer, and it may take place in a much slower regime, as discussed in the next section. In summary, even if other conformations of the dimer cannot be ruled out as contributors to the transient absorption, those related to the face-to-face arrangement seem to better qualify as preferential structures for the homodimer excimer.

F. Adenine Excimer Deactivation Process. The described CASPT2 calculations on the adenine homodimer enable us to propose the model displayed in Figure 5 for the decay dynamics of oligomers of stacked adenine molecules. It can be assumed that at the moment of the absorption the system acquires an exciton-type excited form which rapidly will evolve toward the formation of favorable excimer states in the lowest singlet excited state. Long-lived signals in dinucleotides are indistinguishable from ones in longer homoadenine sequences, indicating that a common excimer state spanning two stacked bases is formed in all systems.¹⁶ The initial excitation (250 nm, 4.96 eV in the fs-ESA experiments^{7,11}) is then expected to take place between the computed 5.25 eV of the S_1 monomer absorption and that corresponding to the major B-DNA structure (5.14 eV, vertically, and 4.80 eV, adiabatically). As previously proposed,^{15,16} from this moment two main decay pathways can be envisaged, and the predominance of one or the other will depend on the balance between the forces that lead to a strong interaction of the stacked nucleobases and the mechanical forces involved in the inherent flexibility of the oligomer (DNA) strands. The system might then either adopt two basic types of conformation differing in the structure of the stacking. More stacked arrangements of the excimer (in which the overlap of the π structures and the corresponding

(56) Marguet, S.; Markovitsi, D. *J. Am. Chem. Soc.* **2005**, *127*, 5780–5781.

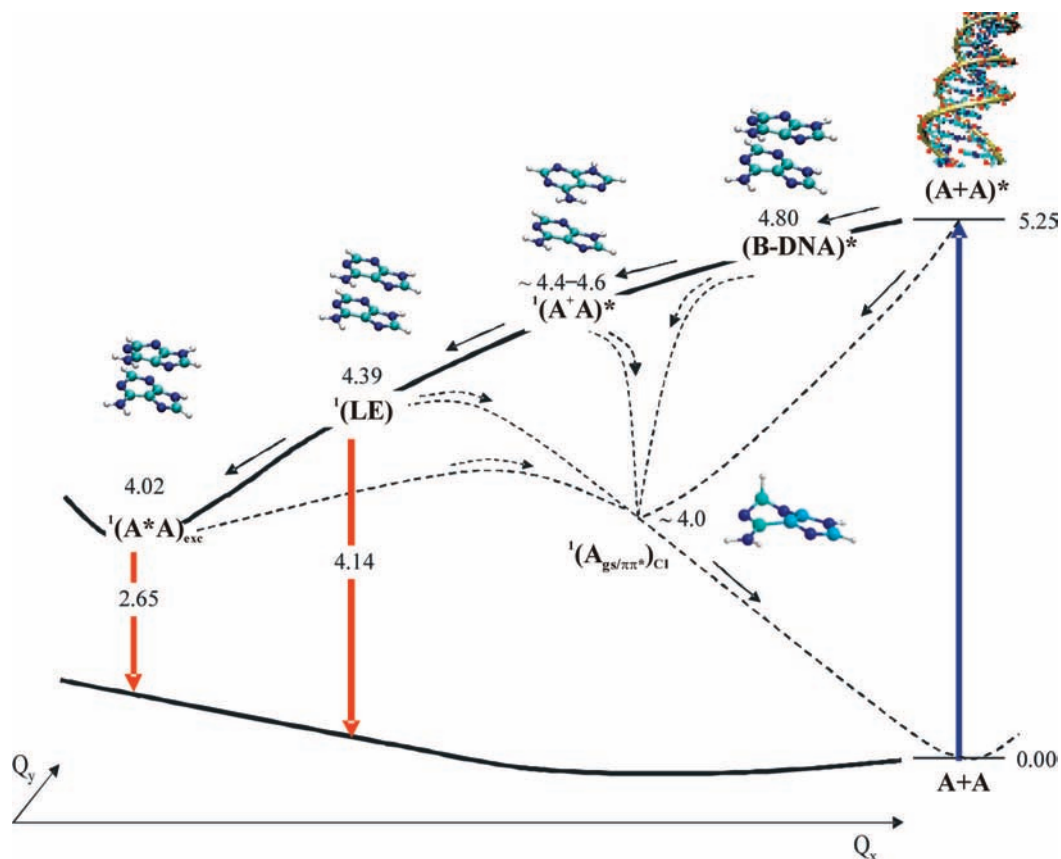


Figure 5. Scheme proposed, based on actual CASPT2 results, for the decay path of the lowest singlet excited state (S_1) of the adenine dimer involving several conformations of the excimer and the adenine monomer conical intersection ($gs/\pi\pi^*$)_{Cl}. The values of the relative energies are in eV. This is a scheme of energy levels. Evolution on the S_1 hypersurface from the initially photoinduced structures toward the different excimer arrangements will not require passing sequentially through each one of the represented conformations. The Q_x coordinate is mainly related to the average intermolecular distance of the two moieties, whereas Q_y is associated to the remaining degrees of freedom in the monomer and the dimer.

binding interaction increase) might decay in an ultrafast manner toward more favorable interacting excimer structures. On the other hand, in cases with minor stacking (minor overlap and binding) or basically unstacked bases, the dimer can localize its population in one of the moieties and undergo an ultrafast decay to the ground state through the well-known conical intersection of the monomer, ($gs/\pi\pi^*$)_{Cl}, located at the CASPT2 level near 4.0 eV (see Figure 5).^{4,5} This relaxation path for the unstacked nucleobases has been found dominant in the decay dynamics of dinucleotides after excitation at 267 nm (4.96 eV); therefore, it reflects the behavior of the dynamics in the blue transient region¹¹ and can be assigned with a lifetime ~ 2 ps as the rate-limiting step of vibrational energy transfer to the environment.¹⁶ Notice that Figure 5 has to be understood as a scheme of energy levels. Evolution on the S_1 hypersurface from the initially photoinduced structures toward the different excimer arrangements will not require passing sequentially through each one of the represented conformations.

Thanks to the inherent flexibility of DNA that allows large-scale nuclear motions and the favorable interactions that lower the excited-state energy, the degree of overlap and stacking of the excimers can increase and the dimer can evolve toward more stable situations. It has been hypothesized¹⁶ that the dimer reaches a charge separated excimer conformation (A^+A^-)* from which most part of the excimer emission is produced. A correlation has been found for distinct heterodinucleotides between the measured lifetimes case of the adenine homodimer.

We have found that the CT states are not the most stable excimer conformations, even in aqueous solutions, as discussed in previous sections. This fact does not imply that they cannot be reached in important amounts, because the evolution of the system and the yield of formation of the different arrangements in the excimer state depend also of the capability of the strand to adopt a favorable position for proper stacking. Moreover, the situation may be quite different in NAB heterodimers, not only because of the degree of overlap and stacking can be expected to be much lower but also because the charge recombination force will be more favorable than in homodimers, in particular for pairs of purine and pyridine bases, which easily compensate for their better donor and acceptor characters, respectively. In the homodimers, however, we have found that the face-to-face conformations (twisted 36° from the B-DNA form⁵³), which maximize the overlap of the π clouds, give rise to much more stable excimer situations, and it can be expected that they can be reached in noticeable quantities. The good correspondence of the computed and the experimental transient absorption spectrum described in subsection E also support such conclusion. Those conformations, in particular $^1(A^*A)_{exc}$, are analogous to those acquired by the cytosine⁴³ and thymine⁵¹ homodimers and that are precursors of the formation of the cyclobutane pyrimidine dimers, whose yields of formation have been found in significant amounts.^{9,57} As found in a recent CASPT2 study,⁵¹ these structures play a different role in the

(57) Douki, T.; Cadet, J. *Biochemistry* **2001**, *40*, 2495–2501.

thymine and the cytosine homodimers. Even when the same type of excimer interaction is what favors the formation of the CI in the excited state, the thymine excimers are probably just intermediate short-lived conformations leading to a lower-lying CI structure and a corresponding ultrafast (1 ps⁹) and high quantum yield TT cyclodimer formation.⁵⁷ On the other hand, for the cytosine dimer they represent structures more stable than the CI, decreasing the yield and enlarging the state lifetime in the formation of CC, as found in experiment.⁵⁷ In the A homodimer, the absence of cyclodimer formation should be made to consider ¹(A*A)_{exc} as long-lived conformations, such as for the cytosine homodimer. In the case of adenine, the excimer emission energies can be expected to be within the range 4.14 eV, vertical from ¹(LE) down to 2.65 eV, vertical from ¹(A*A)_{exc} within the domain of the suggested excimer emission (4.0–2.3 eV),¹¹ and considerably red-shifted with respect to the monomer fluorescence (4.5–4.8 eV).^{5,46–50}

Once the excimer structure has been reached, the decay toward the ground-state should be much slower. The main channel for internal conversion in the adenine homodimer is the conical intersection of the monomer, (gs/ππ*)_{CI}, placed near 4.0 eV, that is almost isoenergetic with the most stable excimer structure ¹(A*A)_{exc}. As the excimer is a minimum in the potential energy surface cut on S₁, a barrier can be predicted in the decay path toward the CI, which can be attributed to the process of releasing the stacking interaction (by increasing the intermonomer distance as the main coordinate modulating the extent of binding character in the excimer) and localization of the excitation in one of the monomers. Such types of barriers, with different heights, can be expected in all paths connecting the excimer surface with the CI funnel. It is therefore plausible to attribute the lifetime measured from 103 to 182 ps in different adenine oligomers^{7,11,16} to the deactivation of the singlet excimer to the ground state, and also to support the idea of several decay channels for different excimer minima controlling the dynamics of the visible ESA region,¹¹ among them the decay by charge recombination. The results obtained for the system in water do not change the overall scheme, even when the relative stabilization of the CT states is larger (~0.2–0.3 eV) than that undergone by the non-CT states (<0.1 eV) (cf. Table 2 and text). In the polar environment and within the oligonucleotide strand it is however possible that the participation of the CT states increases.

For other NABs heterodimers the decay lifetimes have been reported ranging from 10 to 100 ps.¹⁶ Recent fs-ESA experiments performed in strands of alternating (d(GC)₉) and partially nonalternating (d(C₄G₄), d(C₅T₄G₅), d(C₅A₄G₅)) oligomers¹⁵ show how the latter decay much more slowly, what can be clearly attributed to the predominance of homodimer stacking, a promoter of stronger interaction, and lower-lying excimer states with larger lifetimes. The importance of the CT excimers can be expected to decrease in these cases. Finally, it is worth remembering that especially in pyrimidine dimers, new channels for deactivation will be open toward the formation of dipyrimidine adducts like those described recently for the production of cyclobutane cytosine and thymine homodimers.^{6,51} In the case of the cytosine dimer the corresponding conical intersection was computed at 3.5 eV, competitive with the monomer CI, at 3.6 eV, and slightly higher than the ¹(C*C)_{exc} excimer state at 3.3 eV. For thymine, on the contrary, the CI leading to the formation of the adduct was found near 3.3 eV, much lower than the ¹(T*T)_{exc} excimer state at 3.6 eV and the monomer CI at 3.9

eV, rationalizing in this way the higher formation yield found in thymine than in cytosine adducts.^{6,51} At least for those systems involving pyrimidine nucleobases additional paths for deactivation will take place via the triplet manifold, and their importance will rely on the degree of spin–orbit coupling.⁶

Summary and Conclusions

The major goal of the present research is understanding the role that adenine excimers play in the photophysics and photochemistry of adenine oligonucleotides. Our calculations on the adenine homodimer, together with our previous studies on the nucleobases pyrimidine homodimers,^{6,51} support the idea that the long-lived excited states seen in DNA model systems are of excimer (exciplex) type, that is, formed by stacks of two nucleobases, and that they are the origin of the red-shifted fluorescence observed in different oligonucleotides.^{3,11–14} The flexibility of DNA is crucial for the formation of the excimer because the degree of coupling between the two moieties, and therefore the stability of the excimer conformation, will rely on the accessible orientation in the DNA strand. We have presented here two extreme cases, the B-form DNA structure where the overlap for the two adenine monomers is limited, and the ¹(A*A)_{exc} excimer where the interaction is maximum. Intermediate to those two structures we have located charge transfer excimer states whose importance and yield of formation is expected to vary in the sequence of nucleotides depending on the driving force controlling the charge separation between the pair of bases. Such driving force is not expected to largely increase from that of the nucleobase in the biological environment where the nucleotide is surrounded with counterions.⁵⁸ The evolution of the system can be understood from an initial bifurcation between stacked and unstacked nucleobase pairs, which may decay in an ultrafast manner (in a sub-picosecond regime) toward the formation of excimer states or the ground state, respectively, the latter channel being open through the presence of the conical intersection between the S₁ and S₀ states of the monomer, (gs/ππ*)_{CI}. The formed excimer states will, on the other hand, display weak fluorescence and much slower decay times (from tenths to hundred of ps) to the ground state once the barrier to reach the CI of the monomer has been surmounted, a barrier that will be basically related to the energy required to separate the interacting moieties. Additional channels for deactivation will be accessible for pyrimidine dimers with the formation of nucleobase adducts like the cyclobutane pyrimidine dimers through a corresponding conical intersection or singlet–triplet crossing.^{6,51}

It is clear therefore that DNA dynamics (see ref 59 for a recent review), its photophysics and photochemistry, will be controlled to a large extent by the formation of excimers/exciplexes, that is, nucleobase excited dimers, and also that the yield in which these excited dimers will be reached will strongly depend on the conformational properties of the DNA strand and the possibility of generating reactive orientations. Intrastrand stacking interactions seem in this way more relevant than interstrand proton/hydrogen interactions to explain the relaxation dynamics of DNA, which in this way presents slow decay pathways not existent in the monomer

(58) Rubio, M.; Roca-Sanjuán, D.; Merchán, M.; Serrano-Andrés, L. *J. Phys. Chem. B* **2006**, *110*, 10234–10235.

(59) Middleton, C. T.; De La Harpe, K.; Su, C.; Law, Y. K.; Crespo-Hernández, C.; Kohler, B. *Annu. Rev. Phys. Chem.* **2009**, *60*, 217–239.

nucleobases. The relevance of the different excimer/exciplex conformations (face-to-face, charge transfer) in the photochemistry of the different sequence of nucleobases will have to be studied in the future from a theoretical viewpoint, in particular in the formation of exciplexes.

Acknowledgment. Financial support is acknowledged from projects CTQ2007-61260 and CSD2007-0010 Consolider-Ingenio in Molecular Nanoscience of the Spanish MEC/FEDER.

Supporting Information Available: Additional details on the basis set superposition error correction, BSSE-uncorrected curves, solvation model, and Cartesian coordinates of all the structures. This material is available free of charge via the Internet at <http://pubs.acs.org>.

JA808280J